Supporting Information

for

Optimizing the relaxivity at high fields: systematic variation of the rotational dynamics in polynuclear Gd-complexes based on the AAZTA ligand

Lorenzo Tei,[a] Giuseppe Gugliotta,[a] Davide Marchi,[a] Maurizio Cossi,[a] Simonetta Geninatti Crich,[b] Mauro Botta*[a]

[a] Universita' del Piemonte Orientale "Amedeo Avogadro", Dipartimento di Scienze ed Innovazione Tecnologica, Viale T. Michel 11, 15121, Alessandria, Italy. e-mail: *mauro.botta@uniupo.it*

[b] Università di Torino, Department of Molecular Biotechnology and Health Sciences and Molecular Imaging Center, Via Nizza 52, 10125, Torino, Italy.

Contents:

1) General experimental conditions

All reactants were used as supplied from commercial sources unless stated otherwise. Reactions requiring exclusion of moisture were carried out under an argon atmosphere. Water refers to high purity water with conductivity of 0.04 μScm^{-1}, obtained from the "MILLI-Q" purification system.

^{1}H and ^{13}C NMR spectra were recorded on JEOL ECP 400 (^{1}H at 399.968, ^{13}C at 100.572 MHz) spectrometer.

The HPLC analysis and separation was carried out on a Waters system equipped of Waters 1525 binary HPLC Pump, Waters Fraction Collector III and Waters 2489 UV/vis detector. The stationary phase used was the Waters XTerra RPC18 150x4.6 mm column (5μm) (flow rate 1ml/min).

The water proton longitudinal relaxation rates of aqueous solutions of the various compounds were measured by using a Stelar Spinmaster spectrometer (Mede, Italy) operating at 0.5 T and 298 K. The concentration of Gd^{III} in the solution was determined by Evans experiment. For the measurement of the relaxation rates, the standard inversion-recovery method was employed (16 experiments, 2 scans) with a typical 90° pulse width of 3.5 ms, and the reproducibility of the T_1 data was ± 0.5%. The temperature was controlled with a Stelar VTC-91 airflow heater equipped with a copper-constantan thermocouple (uncertainty of ± 0.1 °C). The proton $1/T_1$ NMRD profiles were measured on a fast field-cycling Stelar SmarTracer relaxometer over a continuum of magnetic field strengths from 0.01 MHz to 10 MHz (0.00024 to 0.25 T). The relaxometer operates under computer control with an absolute uncertainty in $1/T_1$ of ± 1%. Additional data points in the range 15-70 MHz (0.37-1.75 T) were obtained on a Stelar Spinmaster console connected to WP-80 magnet (80 MHz (2 T)).

The phantom imaging experiments were carried out on Aspect M2 (Netanya, Israel) MRI instrument operating at 40 MHz (1T) and equipped with a 35 mm coil.

2) HPLC method and retention times

Solvent A: H_2O TFA 0.1%

Solvent B: MeOH TFA 0.1%

Flow: 1 ml/min

Table 2. HPLC gradient conditions

Time (min)	Solvent A (%)	Solvent B (%)
0	90	10
2,50	90	10
15,00	30	70
17,50	0	100
25,00	0	100

Table 3. HPLC retention times for multimeric ligands

Compound	Retention time (min)
L2	13,52
L3	13,89
L4	14.93
L6	13.70
L8	13,90

3) Relaxometric data analysis

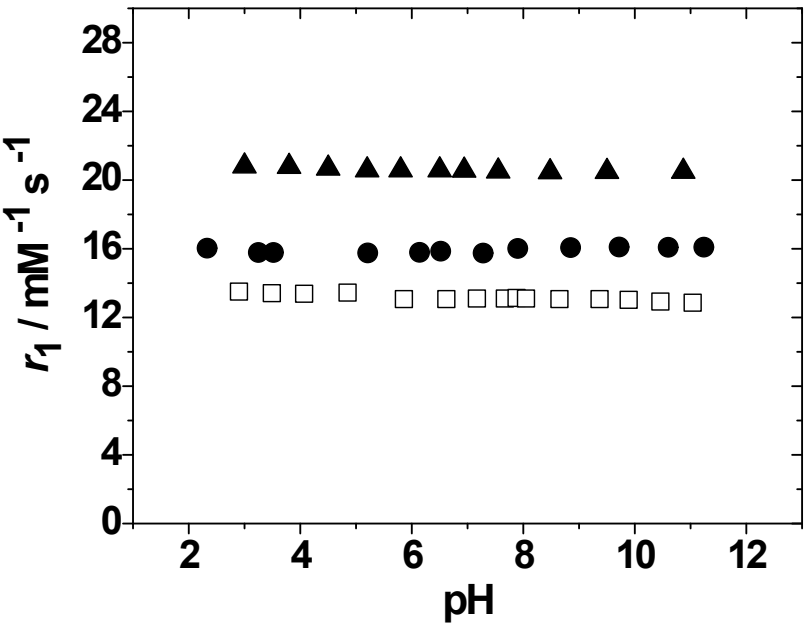

Figure S1. Plots of the ^{1}H relaxivity for [Gd_2**L2**$(H_2O)_4$] (empty squares), [Gd_3**L3**$(H_2O)_6$] (black circles) and [Gd_4**L4**$(H_2O)_8$] (black triangles) as a function of pH.

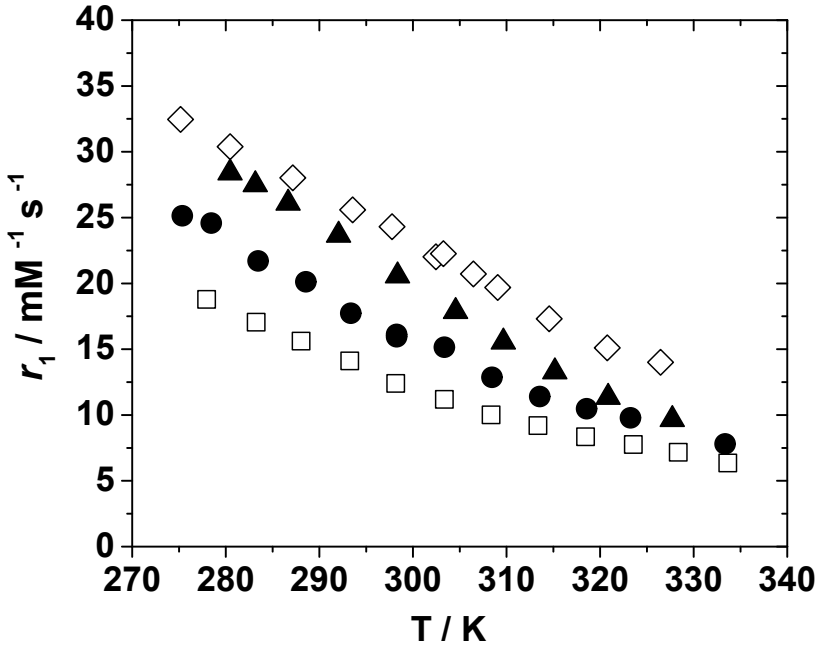

Figure S2. Plots of the ^{1}H relaxivity for [Gd_2**L2**$(H_2O)_4$] (empty squares), [Gd_3**L3**$(H_2O)_6$] (black circles), [Gd_4**L4**$(H_2O)_8$] (black triangles) and [Gd_6**L6**$(H_2O)_{12}$] (empty diamonds) as a function of the temperature.

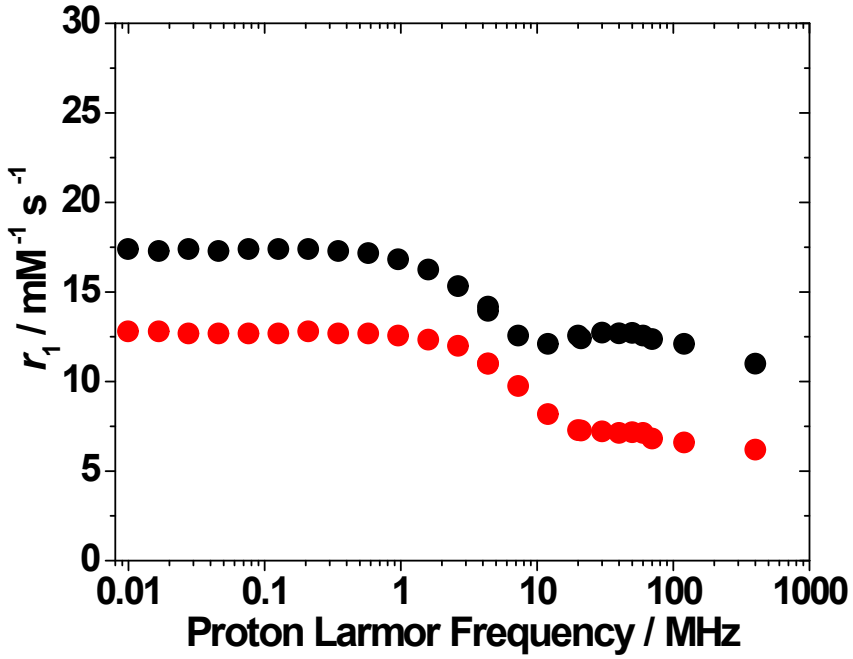

Figure S3. $1/T_1$ ^{1}H NMRD relaxivity data for [Gd_2**L2**$(H_2O)_4$] at pH = 7.0, 298 K (●) and 310 K (●).

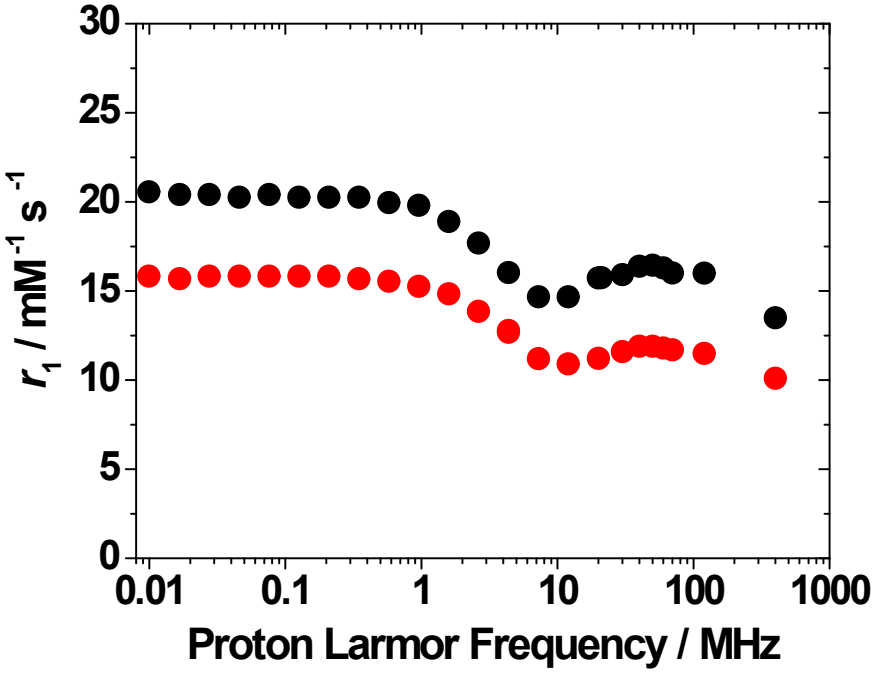

Figure S4. $1/T_1$ ^{1}H NMRD relaxivity data for [Gd_3**L3**$(H_2O)_6$] at pH = 7.0, 298 K (●) and 310 K (●).

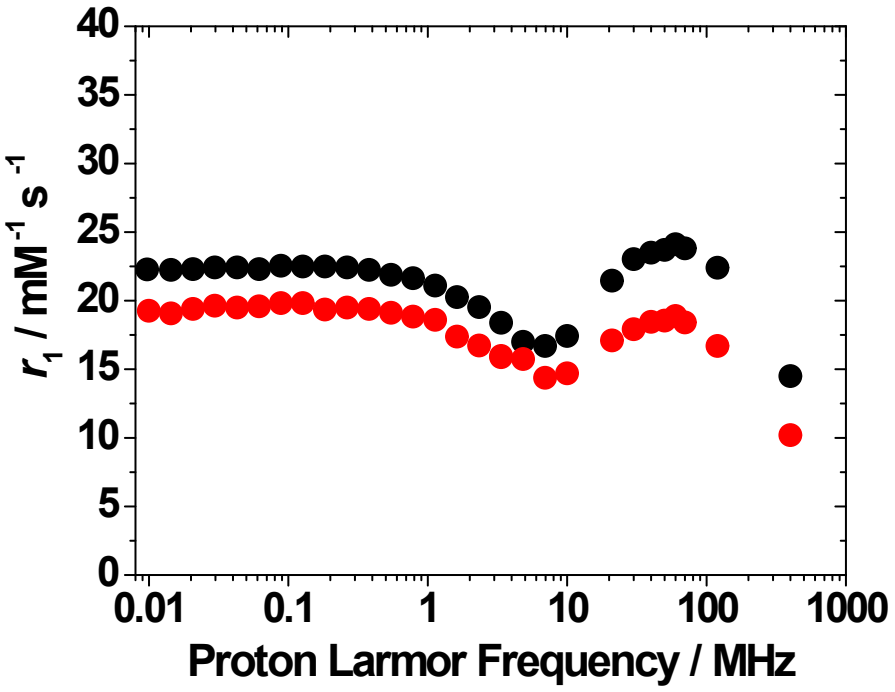

Figure S5. $1/T_1$ ^{1}H NMRD relaxivity data for [Gd_4**L4**$(H_2O)_8$] at pH = 7.0, 298 K (●) and 310 K (●).

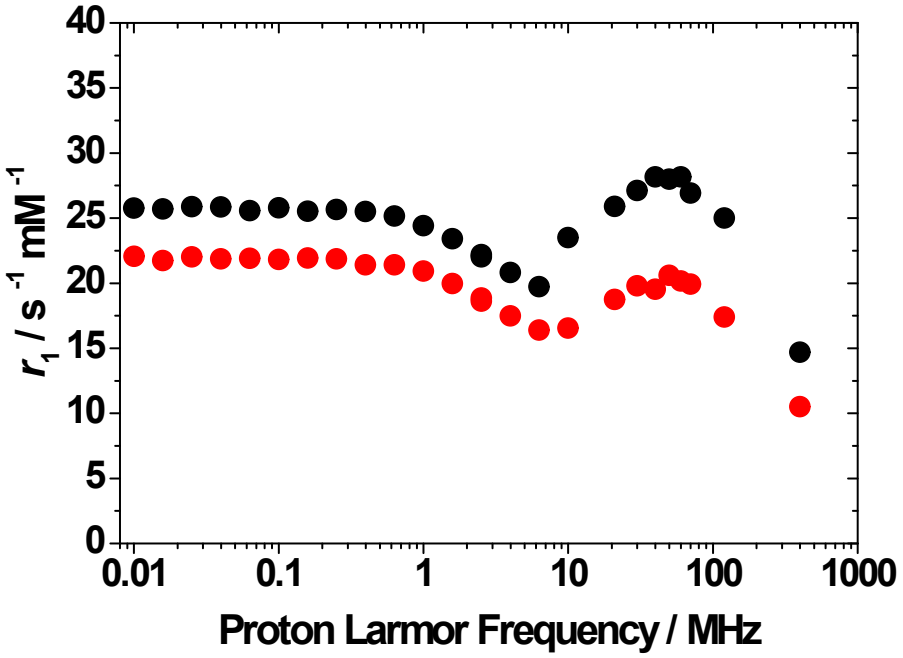

Figure S6. $1/T_1$ ^{1}H NMRD relaxivity data for [Gd_6**L6**$(H_2O)_{12}$] at pH = 7.0, 298 K (●) and 310 K (●).

4) Characterization

(3)

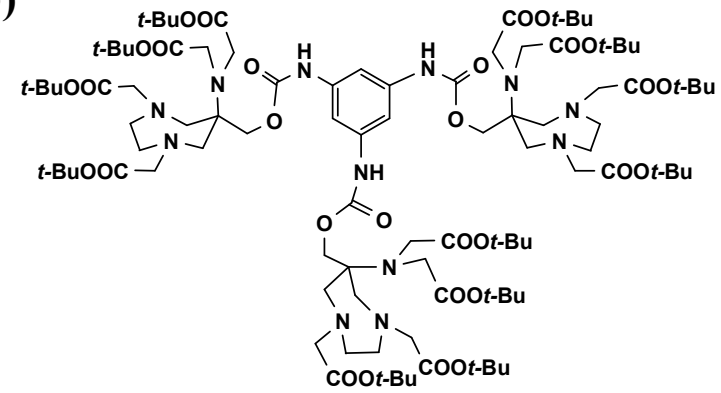

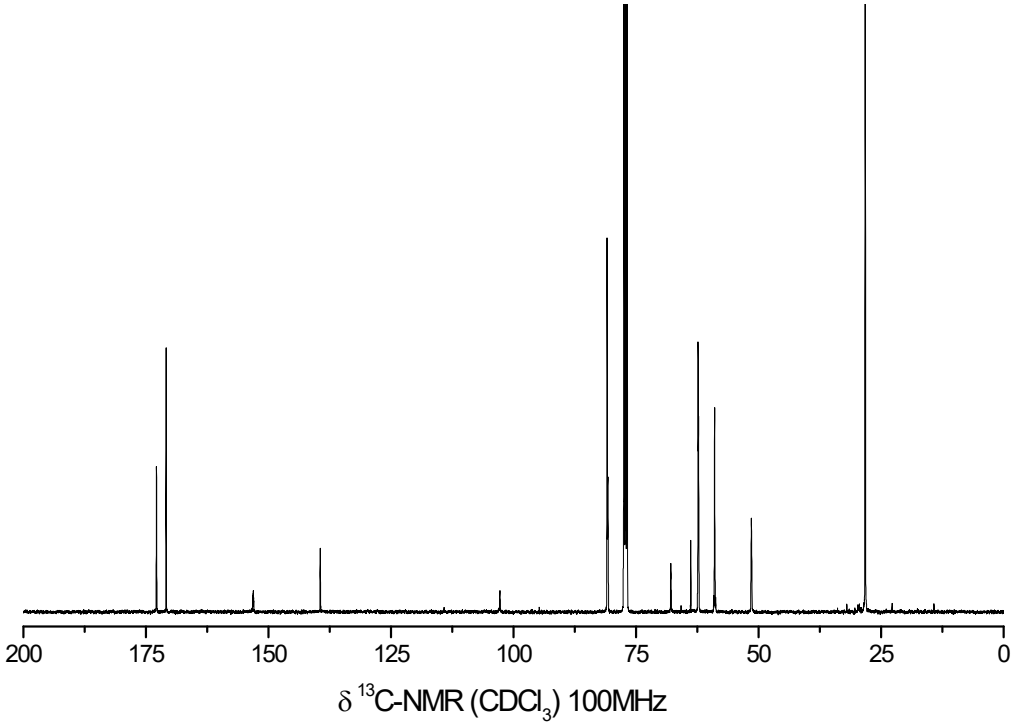

Figure S7. ^{13}C NMR spectrum of intermediate 3.

L3

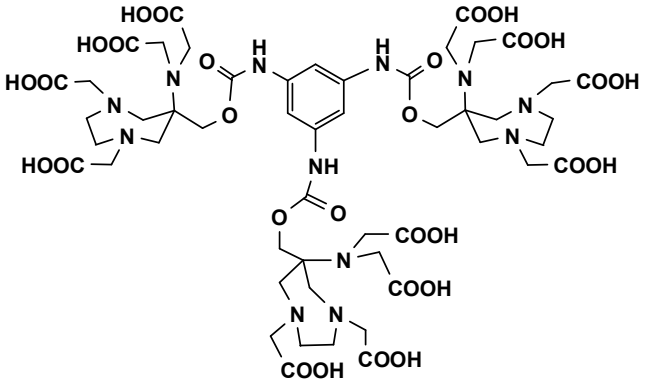

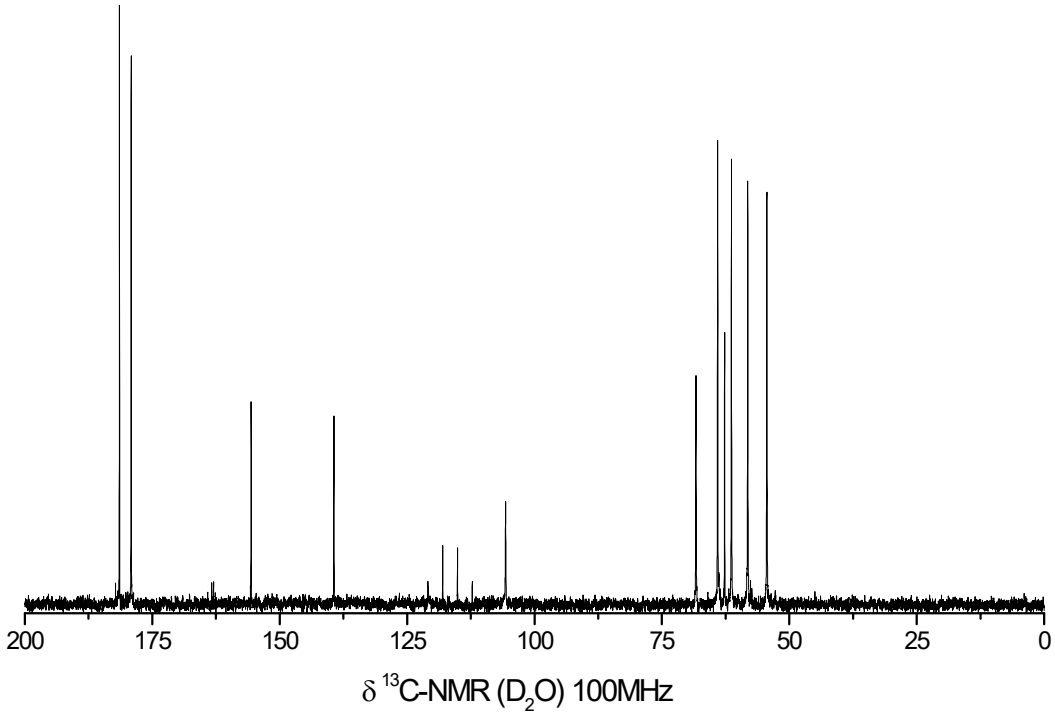

Figure S8. ^{13}C NMR spectrum of trimeric ligand **L3**. Quartets at 116.5 and 163.2 ppm are related to trifluoroacetate anion.

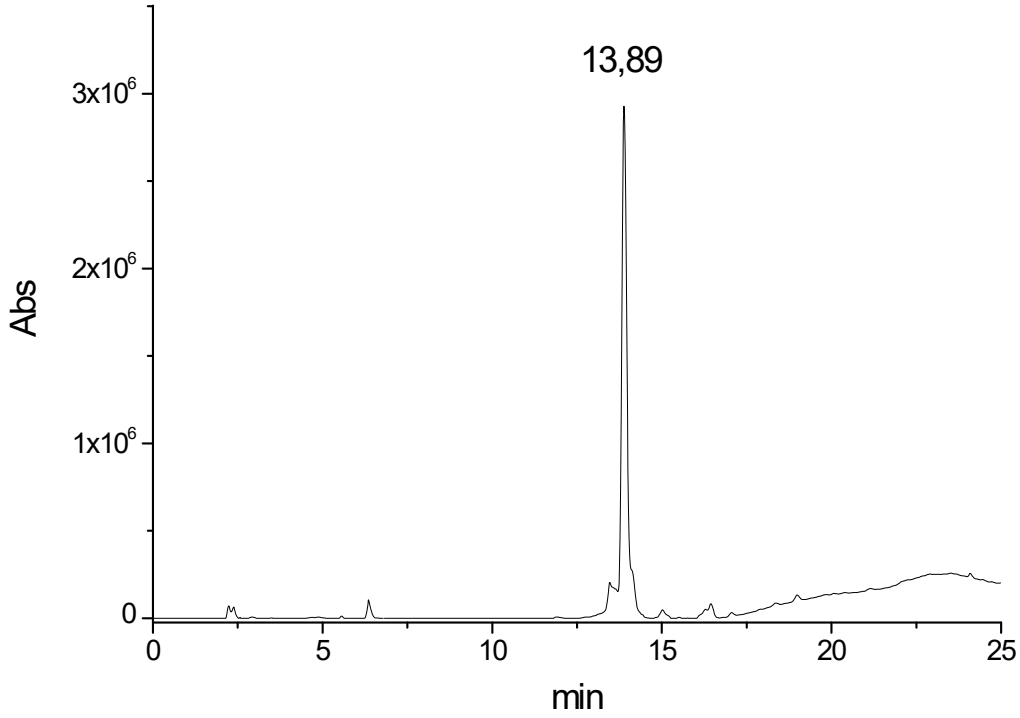

Figure S9. HPLC-UV chromatogram (215 nm) of **L3**.

(4)

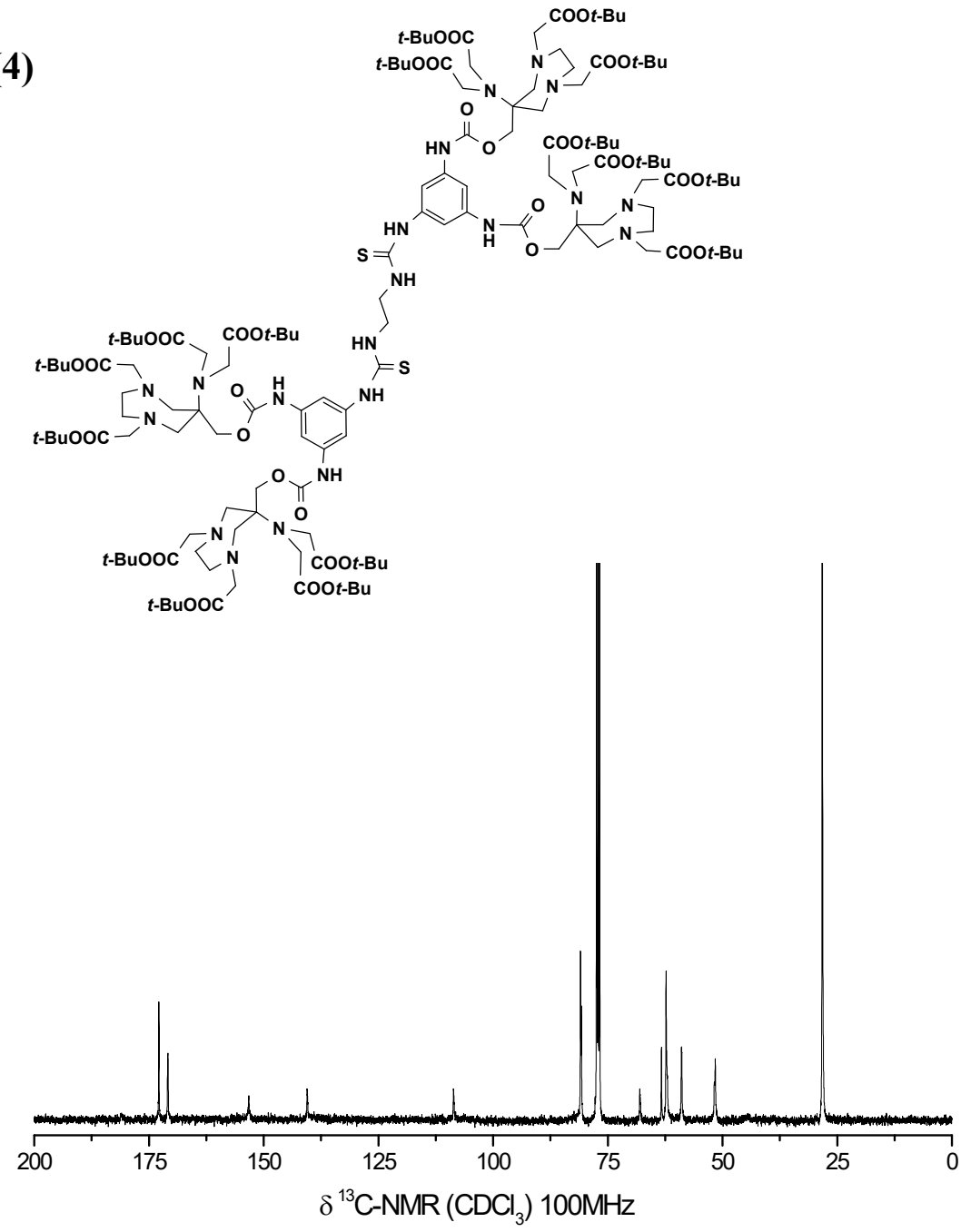

Figure S10. ^{13}C NMR spectrum of intermediate **4**.

L4

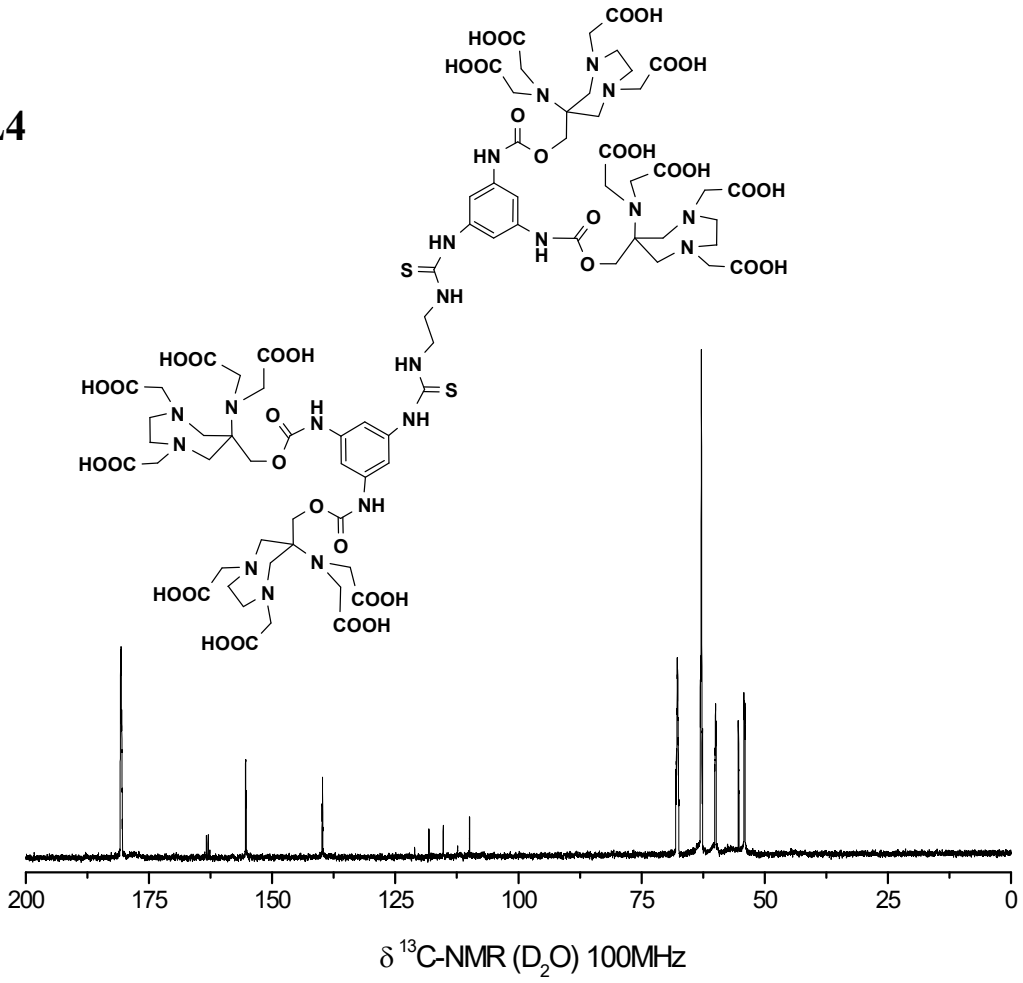

Figure S11. ^{13}C NMR spectrum of tetrameric ligand **L4**. Quartets at 116.5 and 163.2 ppm are related to trifluoroacetate anion.

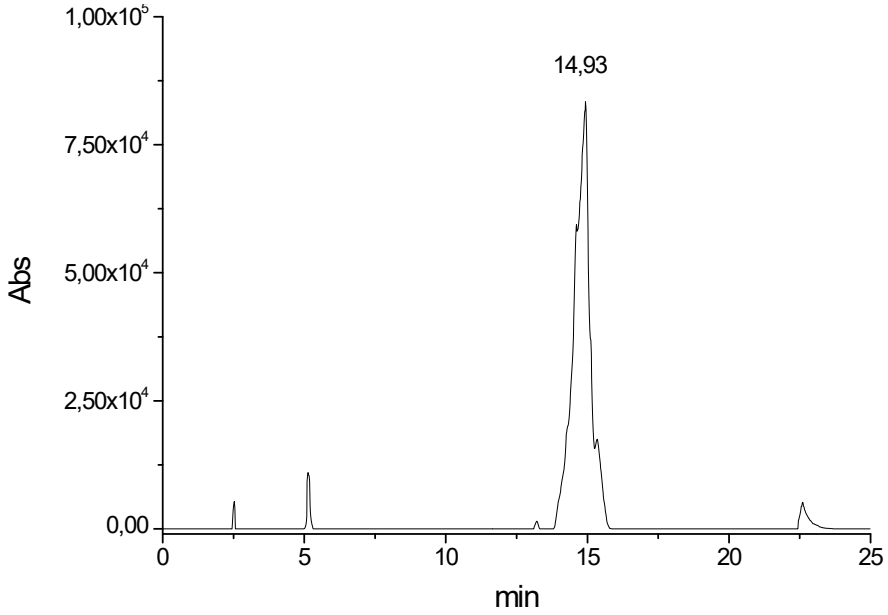

Figure S12. HPLC-UV chromatogram (215 nm) of **L4**.

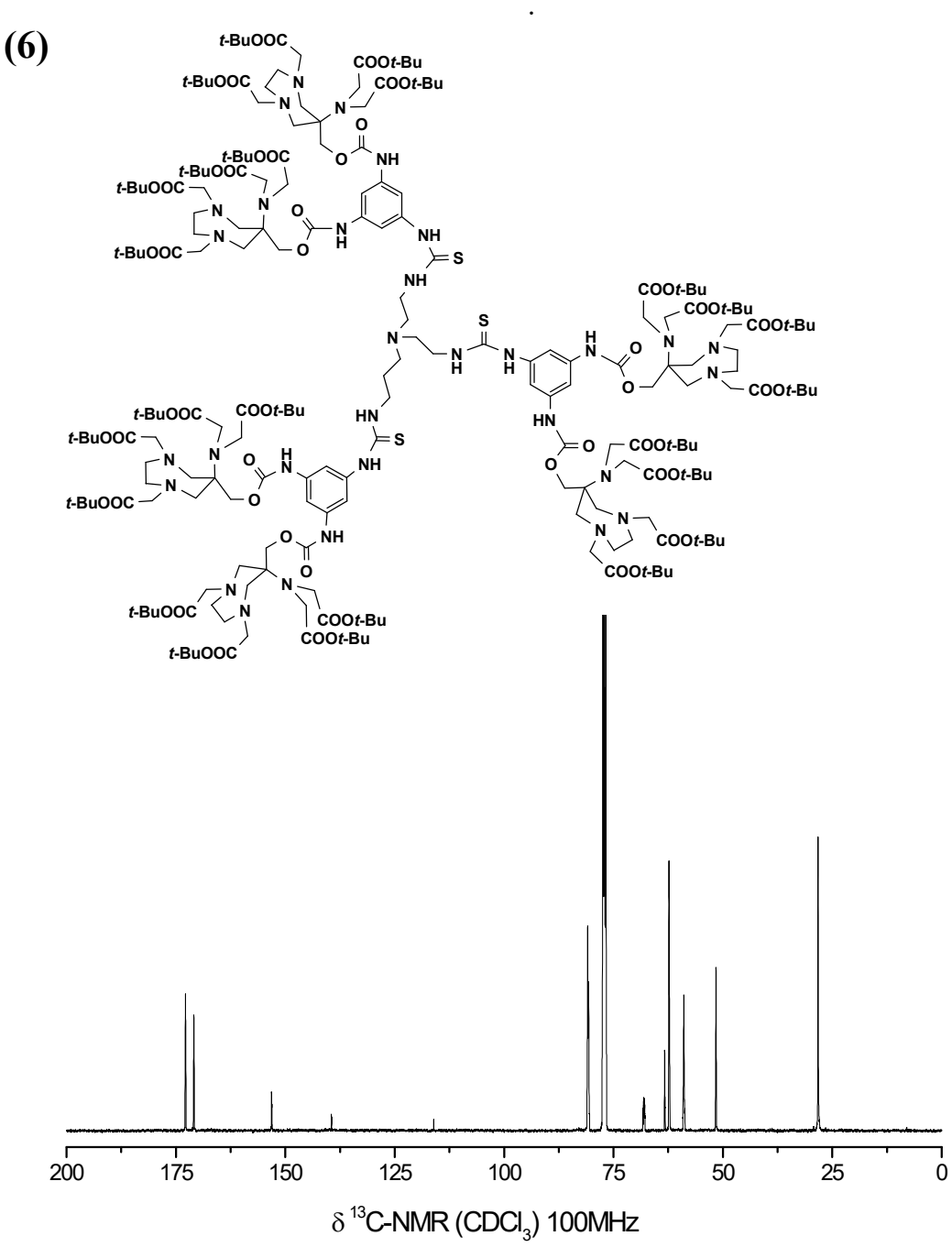

Figure S13. ^{13}C NMR spectrum of intermediate **6**.

L6

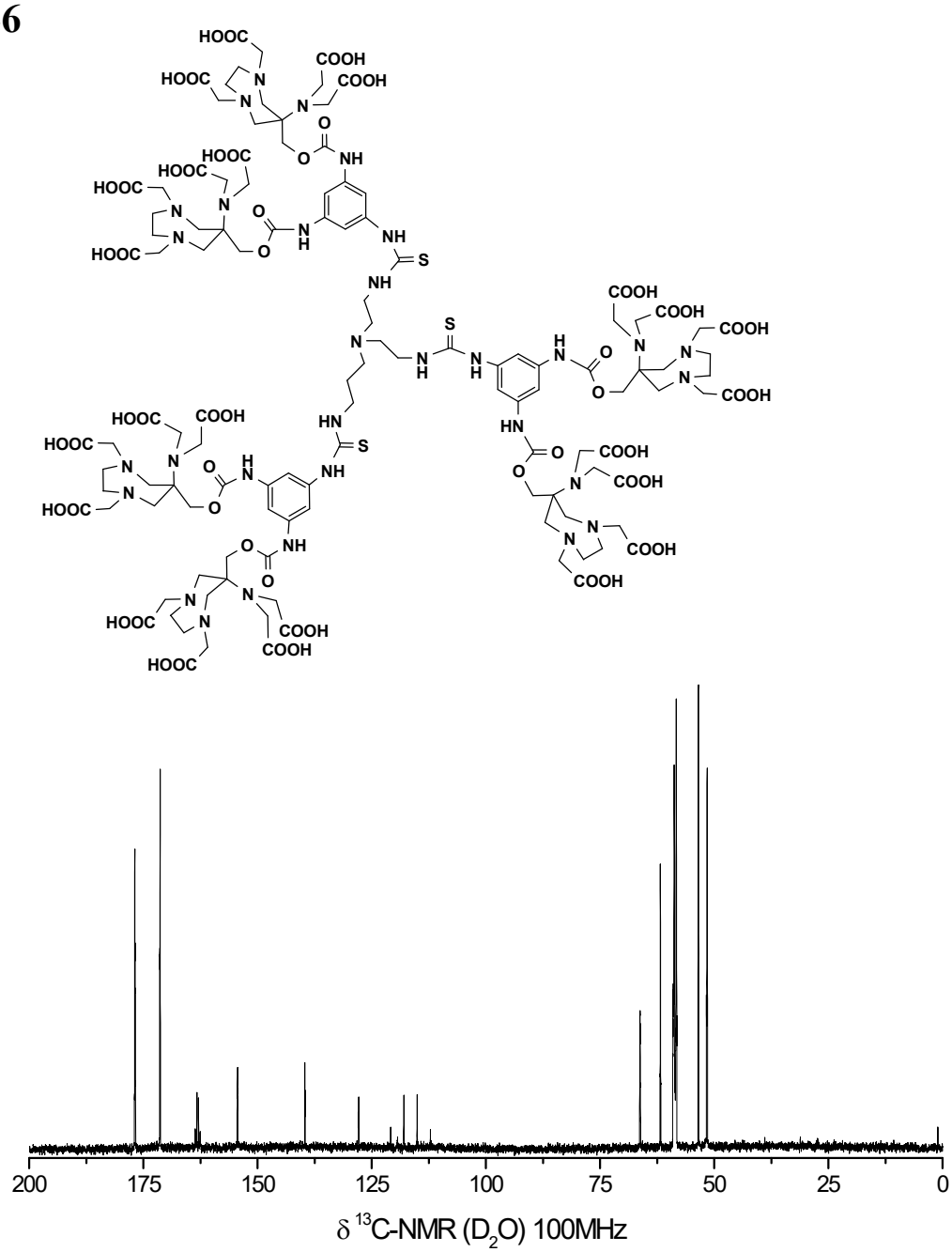

Figure S14. ^{13}C NMR spectrum of hexameric ligand **L6**. Quartets at 116.5 and 163.2 ppm are related to trifluoroacetate anion.

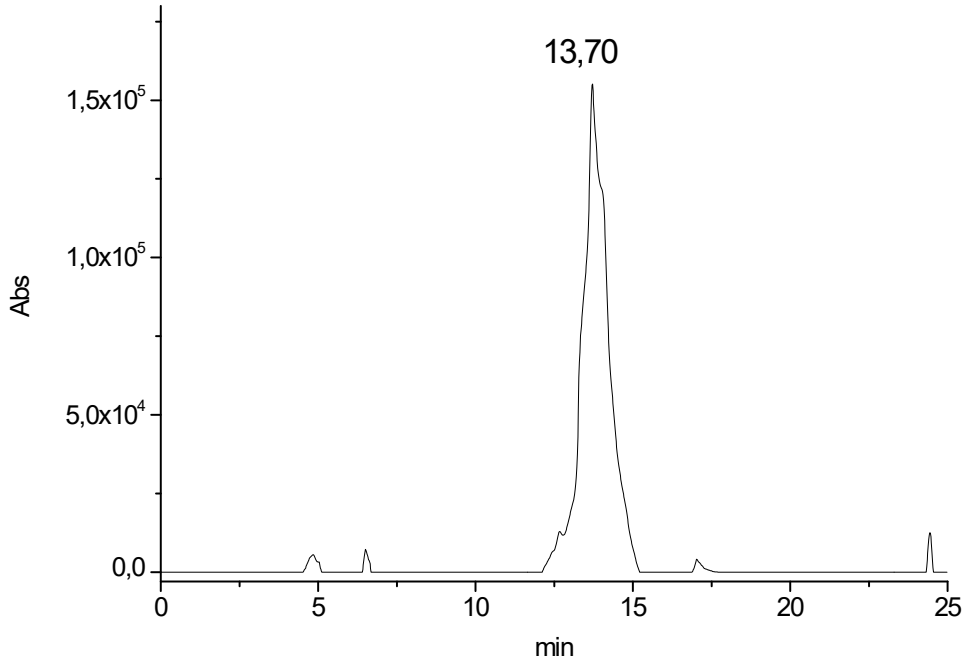

Figure S15. HPLC-UV chromatogram (215 nm) of **L4**.

5) DFT minima

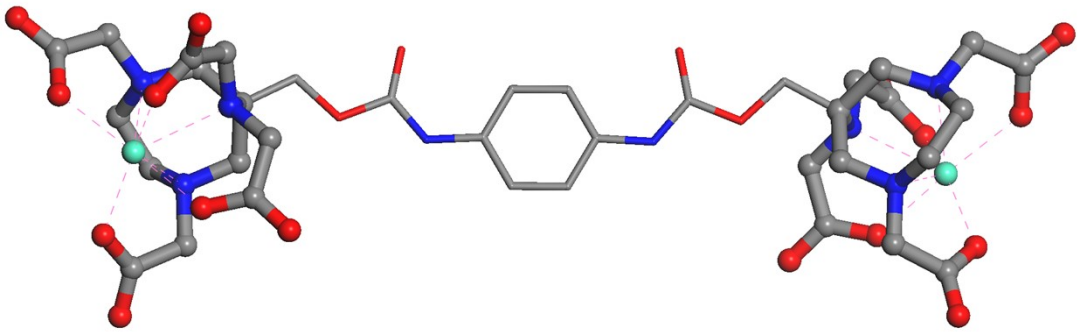

Figure S16. Optimized geometry of Gd_2**L2**.

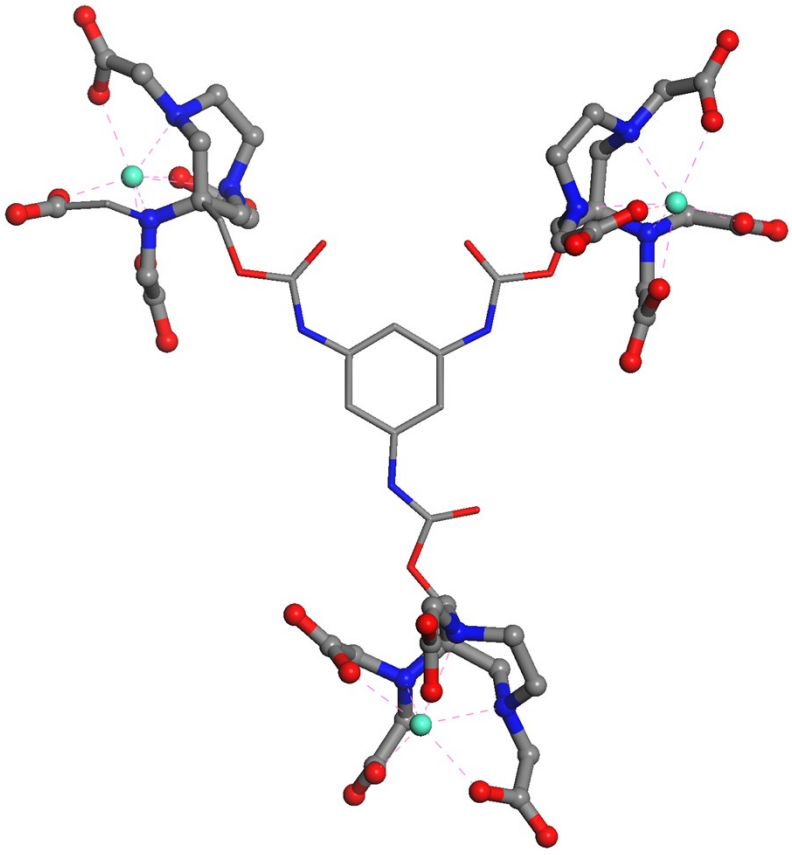

Figure S17. Optimized geometry of Gd_3**L3**.

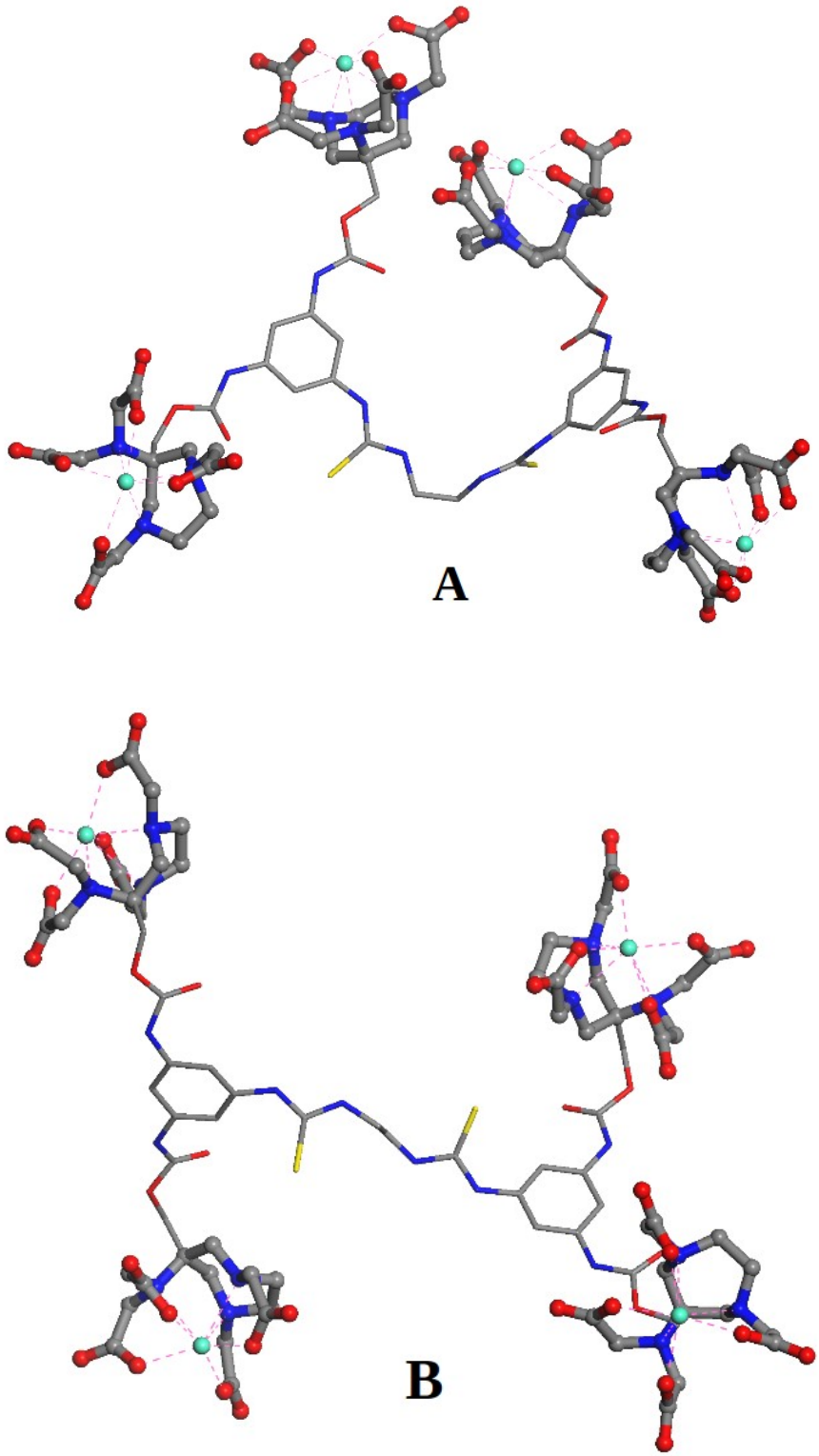

Figure S18. Optimized geometry of Gd_2**L4**. A: “closed” conformation; B: “open” conformation.

6) MRI phantom study.

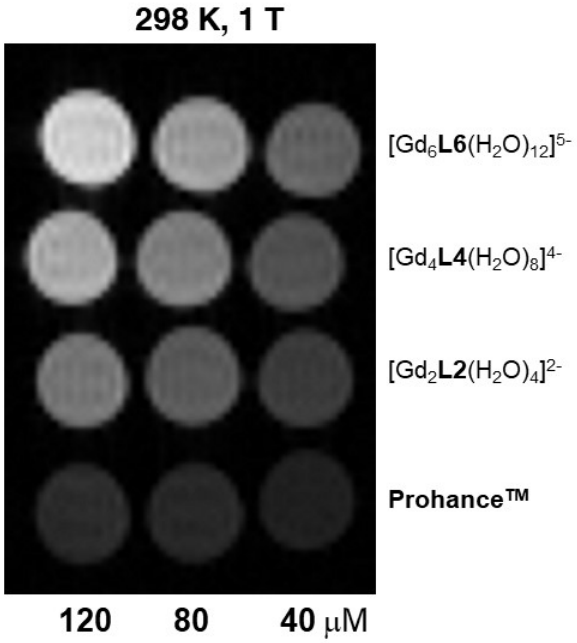

Figure S19. T_1 weighted Multi Slice Spin Echo phantom images (TR/TE/NEX: 250/8/16) recorded at 1 T for solutions of multimers: $[Gd_2\mathbf{L2}(H_2O)_4]^{2-}$, $[Gd_4\mathbf{L4}(H_2O)_8]^{4-}$ and $[Gd_6\mathbf{L6}(H_2O)_{12}]^{5-}$ at 40, 80 and 120 μM concentrations compared to Prohance™ as a control.